Anal Bioanal Chem (2016) 408:4631–4647
DOI 10.1007/s00216-016-9540-x

PAPER IN FOREFRONT

The biochemical origins of the surface-enhanced Raman spectra of bacteria: a metabolomics profiling by SERS

W. Ranjith Premasiri[1,2] · Jean C. Lee[3] · Alexis Sauer-Budge[2,4,5] · Roger Théberge[6] · Catherine E. Costello[6] · Lawrence D. Ziegler[1,2]

Received: 19 February 2016 / Revised: 22 March 2016 / Accepted: 1 April 2016 / Published online: 21 April 2016

Abstract The dominant molecular species contributing to the surface-enhanced Raman spectroscopy (SERS) spectra of bacteria excited at 785 nm are the metabolites of purine degradation: adenine, hypoxanthine, xanthine, guanine, uric acid, and adenosine monophosphate. These molecules result from the starvation response of the bacterial cells in pure water washes following enrichment from nutrient-rich environments. Vibrational shifts due to isotopic labeling, bacterial SERS spectral fitting, SERS and mass spectrometry analysis of bacterial supernatant, SERS spectra of defined bacterial mutants, and the enzymatic substrate dependence of SERS spectra are used to identify these molecular components. The absence or presence of different degradation/salvage enzymes in the known purine metabolism pathways of these organisms plays a central role in determining the bacterial specificity of these purine-base SERS signatures. These results provide the biochemical basis for the development of SERS as a rapid bacterial diagnostic and illustrate how SERS can be applied more generally for metabolic profiling as a probe of cellular activity.

Keywords Surface-enhanced Raman spectroscopy · Bacteria · Nucleotide degradation · Purine metabolism · Metabolic profiling

Electronic supplementary material The online version of this article (doi:10.1007/s00216-016-9540-x) contains supplementary material, which is available to authorized users.

✉ W. Ranjith Premasiri
ranjith@bu.edu

✉ Lawrence D. Ziegler
lziegler@bu.edu

[1] Department of Chemistry, Boston University, 590 Commonwealth Ave., Boston, MA 02215, USA

[2] The Photonics Center, Boston University, 8 Saint Mary's St., Boston, MA 02215, USA

[3] Division of Infectious Diseases, Department of Medicine, Brigham and Women's Hospital and Harvard Medical School, 181 Longwood Ave., Boston, MA 02115, USA

[4] Fraunhofer Center for Manufacturing Innovation, 15 Saint Mary's St., Brookline, MA 02446, USA

[5] Department of Biomedical Engineering, Boston University, 44 Cummington St., Boston, MA 02215, USA

[6] Center for Biomedical Mass Spectrometry, Boston University School of Medicine, Boston, MA 02118, USA

Introduction

Surface-enhanced Raman spectroscopy (SERS) has become a well-established analytical technique that has been exploited in a large number of biomedical applications for the identification of molecular markers of biological activity [1–3]. One recent SERS biomedical application that has generated considerable interest and activity is the use of SERS for the rapid, growth-free detection and identification of vegetative bacterial cells for infectious disease diagnostics [4–12]. SERS offers some unique advantages for bacterial infectious disease identification: extrinsic labeling is not needed, the large signal enhancement permits the rapid, growth-free acquisition of SERS spectra, the method is less susceptible to contamination than nucleic acid amplification techniques, bacterial identification can be achieved by minimally trained personnel with relatively low cost, and portable SERS instrumentation allows point-of-care diagnostics.

The ability to acquire SERS spectra of whole vegetative bacterial cells has been demonstrated by several research groups in the past 15 years [6–8, 11, 12–43]. However, despite the large number of bacterial SERS observations,

interpretation of the observed vibrational signatures in terms of the chemical species and biological basis for these signals has not been achieved, thus limiting the development of this technology for bacterial diagnostics and other whole-cell-based biomedical applications. The purpose of this article is to unequivocally assign the molecular origins of the vibrational features that appear in SERS spectra of bacterial cells, and to identify the cellular mechanisms that account for these species-specific vibrational signatures.

Reported SERS spectra of whole bacterial cells exhibit fairly consistent bacterial SERS spectra for each of the most commonly used excitation wavelengths: approximately 514.5 nm and approximately 785 nm. Normalized SERS spectra of ten representative, strain-specific bacteria excited at 785 nm are displayed in Fig. 1. Bacterial samples were grown to log phase in culture medium, washed with water, and the whole cells were subsequently placed on an Au-nanoparticle-covered SERS substrate [19]. Both gram-positive and gram-negative species are among this set of bacteria. The spectra in Fig. 1 are very similar to those previously reported for the identical organisms and excitation wavelength [4, 6, 8, 11, 16, 18–20, 23, 24, 28–34, 36–42] (Boardman et al. 2016 Rapid detection of microorganisms directly from blood with surface enhanced Raman spectroscopy, unpublished work). A number of vibrational bands are common to the members of this representative set of spectra.

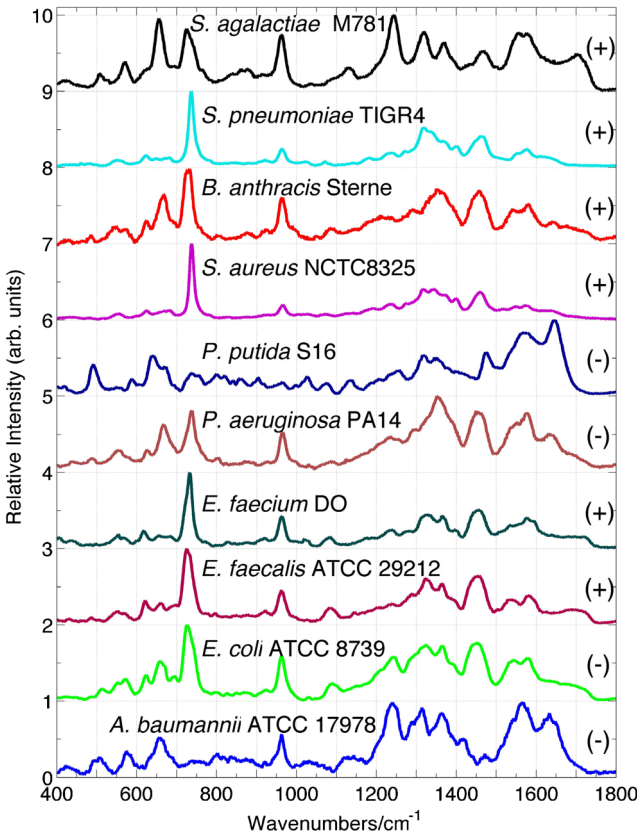

Fig. 1 Surface-enhanced Raman spectroscopy (SERS) spectra of ten bacterial species excited at 785 nm on Au nanoparticle substrates. The spectra are averages of four to six individual spectra and normalized to the intensity of the strongest feature in each spectrum. Gram-positive (*plus sign*) and gram-negative (*minus sign*) types are indicated. See Table 1 for the genus names

A variety of assignments have been previously offered for the observed vibrational features in the SERS spectra of bacteria. Because of the distance dependence of the SERS enhancement mechanisms [49], it has generally been assumed that the observed vibrational bands appearing in the SERS spectra of whole vegetative bacterial cells are dominated by the contributions of their outer cell wall components. Furthermore, the SERS vibrational features of whole bacterial cells are different from the peak frequencies seen in the normal, non-SERS Raman spectra of bacteria, consistent with cell wall molecular components accounting for SERS bacterial signals [19, 35, 50–52]. Correspondingly, the current consensus is that SERS spectra of bacteria are due to a mix of vibrational modes of cell wall components, such as peptidoglycan, lipids, lipopolysaccharides or membrane proteins, and nucleic acids [6, 7, 11, 13, 15–20, 23, 24, 28–33, 37, 38, 40–42], although bacterial SERS spectra do not correlate with cell wall architecture; that is i.e., gram positive versus gram negative (Fig. 1). A few studies have also suggested the possibility that small molecules, such as adenine, may contribute to the observed bacterial SERS spectra as well [11, 16, 33, 39].

The current understanding of these bacterial SERS spectra may be illustrated by the reported assignments for the ubiquitous and generally strongest band observed in SERS spectra of bacteria excited at 785 nm at approximately 725–735 cm^{-1} (Fig. 1). It has been explicitly assigned to the glycosidic ring or C–N stretching mode of *N*-acetyl-D-glucosamine or *N*-acetylmuramic acid, major components of peptidoglycan, a key bacterial cell wall biopolymer [6, 7, 18, 23, 37, 38, 40, 42]. Other proposed assignments for this band include a symmetric O–P–O vibrational mode of the phosphate group [34], adenosine [24], adenine [16], or adenine-containing molecules such as flavin adenine dinucleotide (FAD) or nucleic acids [7, 11, 30, 32, 33, 37–39, 42, 43]. Finally, one bacterial analysis attributed these spectral features to cell culture contaminants [36]. Aside from the expectation based on the distance dependence of the plasmon enhancement mechanism, the main basis for these assignments was the similarity of the Raman band frequency in SERS spectra of model compounds and the observed bacterial spectra.

A further complication for the assignment of the chemical origins of bacterial SERS spectra is the Raman excitation wavelength dependence of these spectra. Spectra of bacteria excited at 514.5 nm (or 532 nm) have been shown to be virtually identical to those of riboflavins, such as FAD, and exhibit no species/strain dependence [12, 21, 22, 25, 26, 29, 35, 43, 53]. FAD is a coenzyme located in bacterial cell walls. These observations stand in contrast to the SERS spectra produced by excitation at 785 nm that exhibit different vibrational features and species/strain dependence. Thus, there is

considerable uncertainty about the biochemical origins of these bacterial SERS signatures.

To maximally exploit the capabilities of SERS for bacterial identification, it is essential to understand the molecular and corresponding biochemical origins of these SERS vibrational signatures. Such information informs the design of optimal bacterial preparation and enrichment procedures from infectious human body fluids so as to provide maximally robust and reproducible SERS signals. It also provides a basis for understanding the capabilities and limitations for diagnostics by this optical approach and is a requirement for the adoption of this novel rapid diagnostic in the medical community. Finally, a biochemical understanding of these cellular molecular markers has the potential to broaden the uses of SERS to other biomedical applications and provide an even larger chemical biology impact beyond rapid, growth-free bacterial diagnostics.

The results reported here unequivocally establish that the SERS spectrum of bacteria excited at 785 nm is due to metabolites of the purine degradation pathway that result from the rapid onset of the bacterial starvation response. This analysis demonstrates the potential of SERS for monitoring real-time exogenous metabolomics and its more general use to address questions in systems biology.

Methods

Bacterial samples and preparation

The sources for most of the bacterial strains used in this study are summarized in Table 1. In addition, *Staphylococcus aureus* 25904 and *Bacillus cereus* 14579 were obtained from ATCC. The *Escherichia coli* BW25113 (CGSC#7636) parent strain and its two mutants, *E. coli* JW3640-1 Δ*ade* (CGSC#10671) and *E. coli* JW1615-1 Δ*add* (CGSC#9376), and another *E. coli* Δ*add* mutant SO0333 (CGSC#5937) and the corresponding parent strain SO003 (CGSC#6925) were acquired from the Coli Genetic Stock Center (Yale University). *E. coli* BD11996 was donated by BD. Bacterial strains were cultivated overnight before subculture in approximately 15 mL of tryptic soy broth (BD) or LB broth (Sigma), harvested during the log phase by centrifugation of 2 mL of culture, and washed four times with 2 mL of deionized Millipore or distilled water. The cell pellet was resuspended in 0.25 mL of water, and 1 μL of the resulting approximately 10^9/mL bacterial suspension was pipetted directly onto the SERS substrate for spectral acquisition. SERS measurements were made after approximately 5 min, when nearly all the water on the SERS substrate had evaporated. The bacterial solution was filtered through a 0.22-μm Eppendorf filter to obtain bacterial supernatant samples. ^{15}N cell culture medium and ^{15}N-labeled, hypoxanthine, and guanine were acquired from Cambridge Isotope Laboratories (Tewksbury, MA, USA). Sodium pyrophosphate decahydrate ($Na_4P_2O_7 \cdot 10H_2O$) was purchase from Sigma-Aldrich and used with out further purification.

SERS substrates

All SERS spectra reported here were obtained with the in situ grown, aggregated-Au-nanoparticle-covered SiO_2 substrate developed previously in our laboratory [19]. Details concerning the production of these SERS active chips and the characterization of their performance for providing reproducible SERS spectra of bacteria have been described. These

Table 1 Best-fit-determined relative (%) purine contributions to bacterial spectra of the ten species in Fig. 1

Organism	Source or reference	Adenine[a]	Hypoxanthine[a]	Xanthine[a]	Guanine[a]	Uric acid[a]	AMP[a]
Streptococcus agalactiae M781	ATCC	8/2	39/56	47/38	6/4	0	0
Streptococcus pneumonia TIGR4	[44]	65/62	0	3/8	0	0	32/30
Bacillus anthracis Sterne	Colorado Serum Company	27/9	45/71	0	28/20	0	0
Staphylococcus aureus NCTC 8325	[45]	75/69	0	0	8/16	0	17/15
Pseudomonas putida S16	[46]	2/0.6	0	12/11	19/14	54/71	12/4
Pseudomonas aeruginosa PA14	[47]	31/13	17/34	11/13	36/32	5/8	0
Enterococcus faecium DO	[48]	41/14	40/70	5/5	14/11	0	0
Enterococcus faecalis 29212	ATCC	21/5	61/80	10/8	8/7	0	0
Escherichia coli 8739	ATCC	14/3	49/54	25/28	13/14	0	0
Acinetobacter baumannii 17978	ATCC	0	0	60/55	10/7	30/38	0

AMP adenosine monophosphate

[a] The first number is the percent contribution of the purine component surface-enhanced Raman spectroscopy (SERS) spectrum normalized by the spectrum maximum the second number is the percent contribution scaled by the relative cross section of the purine component and is thus the relative number of purine component molecules accounting for the SERS signature

substrates are produced by a two-stage reduction of an Au-ion-doped sol–gel which results in small (2–15 particles) aggregates of monodispersed approximately 80-nm Au nanoparticles covering the outer layer of approximately 1-mm^2 SiO_2 substrate.

Spectral acquisition

The bacterial spectra were acquired with an RM-2000 Renishaw Raman microscope with a ×50 objective and with excitation at 785 nm. SERS spectra were obtained with incident laser powers in the 0.2–2-mW range in an illumination time of approximately 10 s. The observed spectra typically resulted from approximately ten bacterial cells within the field of view (approximately 100 μm^2). The 520-cm^{-1} band of a silicon wafer was used for frequency calibration. Peak frequency precision was ±0.5 cm^{-1}.

Data fitting analysis

The GRAMS/AI™ spectroscopy software suite was used to manually baseline correct the experimental SERS spectra. Averaged bacterial spectra were empirically best-fit by adjustment of component contributions from adenine, hypoxanthine, xanthine, guanine, uric acid, and adenosine monophosphate (AMP). Normalized SERS spectra of 20 μM aqueous solutions of these purines were independently obtained for this analytical purpose. Because of the broad SERS spectral baseline variability and some systematic vibrational frequency shifts between the bacterial and purine-only solutions, better fits to the observed bacterial spectra were achieved by this empirical fitting procedure as compared with standard automated best-fitting procedures.

Nano-electrospray ionization mass spectrometry

Between 3 and 5 μL of filtered (0.22-μm filter, Eppendorf) bacterial supernatant was added to an equivalent volume of 0.2 % formic acid in acetonitrile. The resulting mixture was introduced into an LTQ Orbitrap XL mass spectrometer (Thermo Fisher, San Jose, CA, USA) by means of a TriVersa NanoMate system (Advion Biosciences, Ithaca, NY, USA). A low-flow electrospray ionization chip was used as a static emitter to deliver the sample at 20–40 nL/min. The LTQ Orbitrap XL mass spectrometer was operated in the nanospray positive-ion mode with acquisition over a mass range of m/z 80–1000. All mass spectra measured for ions detected in the Orbitrap were recorded with 60,000 resolution at m/z 400. Mass spectra were generated by the averaging of scans over a period of 1–2 min. Mass accuracy was better than 2 ppm.

Results

SERS spectra of some model compounds and bacteria

Initial evidence suggesting the molecular origins of the SERS spectra of vegetative bacterial whole cells excited at 785 nm was provided by comparison of SERS spectra of bacteria and aqueous solutions of some model compounds. For example, as seen in Fig. 2, spectrum a, the *S. aureus* (NCTC 8325) SERS spectrum on the Au substrate closely resembles that of an approximately 10 μM adenine solution, although the SERS spectra are not identical. The *S. aureus* frequencies are only slightly shifted from those in adenine. For example, the most intense band (at 739 cm^{-1}), corresponding to the ring breathing mode transition of adenine, is slightly redshifted to 737 cm^{-1} in the bacterial spectrum.

In contrast to *S. aureus*, the SERS spectra of *Enterococcus faecalis* ATCC 29212 (Fig. 2, spectrum b) and *Acinetobacter baumannii* ATCC 17978 (Fig. 2, spectrum c) excited at 785 nm closely resemble the SERS spectrum of hypoxanthine and xanthine respectively. Other vibrational bands are also evident in the SERS spectra of these bacterial samples, but the contribution of these compounds to their respective bacterial spectra seems evident. Thus, a different purine molecule, either adenine, hypoxanthine, or xanthine, appears to make the dominant molecular contribution to each of the three bacterial SERS spectra shown in Fig. 2.

Isotopic substitution

SERS spectra of *S. aureus* (ATCC 25904) and *Bacillus anthracis* Sterne cultured in (normal) ^{14}N and isotopically labeled ^{15}N culture media are compared in Fig. 3. Redshifted vibrational frequencies are observed for some of the bands in the SERS spectra of the ^{15}N-labeled bacteria. SERS spectra of ^{14}N and ^{15}N-labeled purine bases are also shown in Fig. 3. The 14-cm^{-1} redshift of the approximately 737-cm^{-1} in-plane ring breathing mode and the 20-cm^{-1} redshift of the 965-cm^{-1} ring breathing mode found for the ^{15}N-cultured *S. aureus* SERS spectra are identical, within experimental precision, to the downshifts observed for the SERS spectrum of ^{15}N-labeled relative to ^{14}N adenine (Fig. 3a). This is further evidence that adenine is the molecule responsible for a significant portion of the *S. aureus* SERS spectrum.

The SERS spectra of ^{14}N- and ^{15}N-cultured *B. anthracis* Sterne are compared with computed SERS spectra resulting from a best-fit-determined (vide infra) linear combination of adenine, hypoxanthine, and guanine SERS spectra for each nitrogen isotope in Fig. 3b. This linear combination also matches the observed redshifts seen in the ^{15}N *B. anthracis* Sterne spectrum relative to the corresponding ^{14}N spectrum. The vertical lines in Fig. 3b highlight how the vibrational redshifts, which range from approximately 0 to 22 cm^{-1}, are

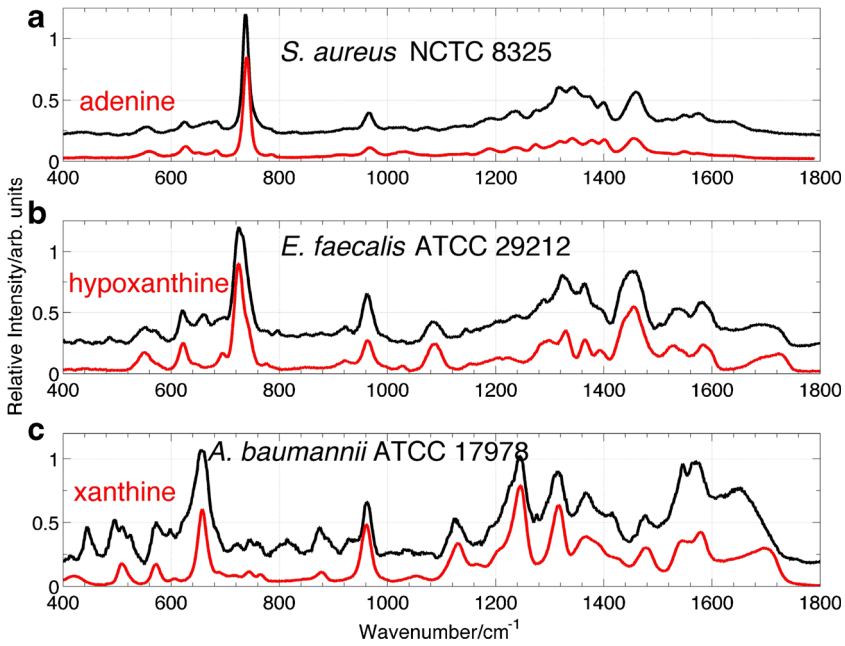

Fig. 2 Comparison of SERS spectra of three bacterial species and some model compounds. The SERS spectra of *Staphylococcus aureus* (NCTC 8325), *Enterococcus faecalis* (ATCC 29212), and *Acinetobacter baumannii* (ATCC 17978) are compared with adenine, hypoxanthine, and xanthine SERS spectra respectively. The SERS spectra of the model compounds are shown in *red*; the SERS spectra of the bacteria are in *black* and have been raised by 0.25 units for viewing convenience. Contributions from these compounds appear dominant in each of these bacterial SERS spectra

captured by the purine-based simulated spectrum for bands at 668, 730, 964, 1358, and 1455 cm^{-1} in the ^{14}N spectrum. These vibrational isotopic shifts are consistent with the largest features in the *B. anthracis* Sterne SERS spectrum being assigned to purine vibrational transitions arising from a combination of adenine, hypoxanthine, and guanine.

Cellular versus supernatant SERS spectra

SERS spectra of four representative bacterial species (*E. faecalis*, *E. coli*, *Bacillus cereus*, and *S. aureus*) and their corresponding enriched supernatants are displayed in Fig. 4. The supernatant was enriched by approximately an order of magnitude on the basis of volume reduction as a result of lyophilization before it was placed on the SERS substrate. As seen in Fig. 4, each of the normalized supernatant spectra is nearly identical to the corresponding bacterial cell SERS spectrum for excitation at 785 nm. Consequently, these pairwise comparisons reveal that these bacterial SERS signatures are *not* due to structural bacterial cell wall features and must arise from small molecules sufficiently water soluble at biological concentrations, which have been secreted from the bacterial cells and collect in the exogenous regions of these organisms. The SERS signals are larger for samples

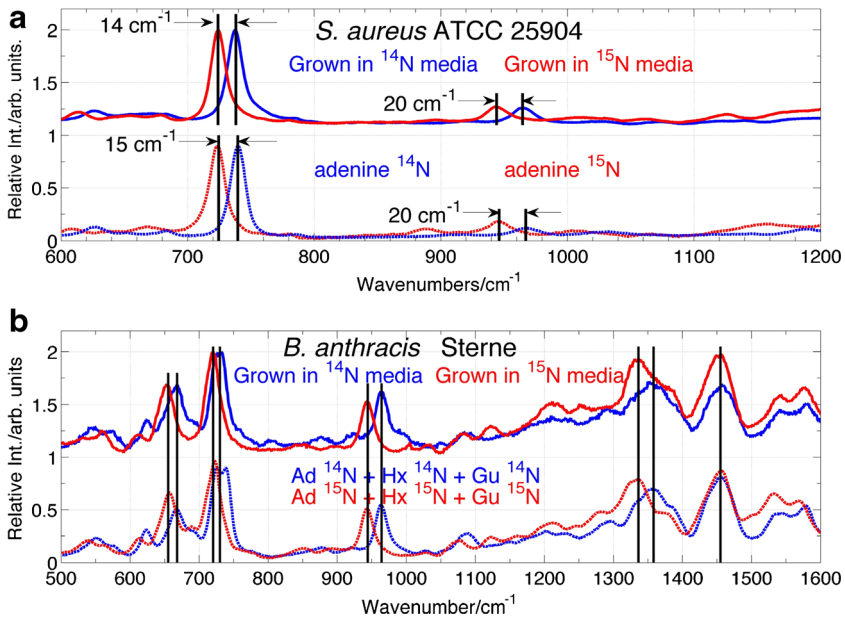

Fig. 3 SERS spectra of *S. aureus* (ATCC 25904) and *Bacillus anthracis* Sterne grown on ^{14}N and ^{15}N growth media compared with ^{14}N and ^{15}N-labeled purines. **a** Experimental ^{15}N isotopic redshifts of *S. aureus* spectra match those observed for ^{15}N-labeled. **b** Observed isotopic redshifts of *B. anthracis* Sterne match those observed for the best-fit-determined linear combination of ^{15}N-labeled, hypoxanthine, and guanine. See the text for more details. *Ad* adenine, *Gu* guanine, *Hx* hypoxanthine

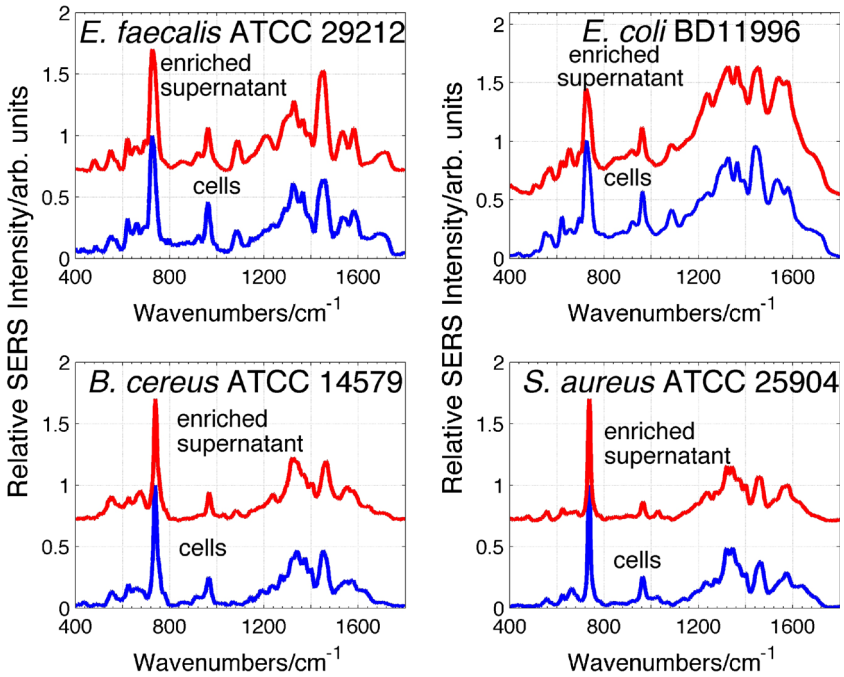

Fig. 4 Comparison of the SERS spectra of four bacterial strains (*blue*) and their corresponding enriched supernatant (*red*). The supernatant was enriched by approximately an order of magnitude before analysis. Each displayed spectrum is normalized by its band maximum, and enriched supernatant spectra are offset for better viewing

containing cells where these molecules must be more highly concentrated (vide infra).

Purine fits to SERS spectra of bacteria excited at 785 nm

Given the preceding evidence suggesting that bacterial SERS spectra are due to small purine-like molecules, each of the observed bacterial SERS spectra shown in Fig. 1 was fit to a linear combination of the SERS spectra of adenine, hypoxanthine xanthine, guanine, uric acid, and AMP. The SERS spectra of 20 μM solutions of these compounds on Au nanostructured substrates excited at 785 nm and normalized to the maximum of the adenine spectrum are shown in Fig. 5. SERS spectra will be especially sensitive to the presence of adenine because of the large relative cross section of its 739-cm^{-1} band (Fig. 5). The peak vibrational frequencies are shifted slightly from those observed in bulk solution Raman (non-SERS) measurements because of interactions with the Au nanoparticle surface and local solvation environment effects, as is well known for SERS [54–56]. SERS frequencies may be even slightly further perturbed relative to SERS spectra of pure aqueous solution potentially because of local pH, ionic strength, or molecular complex formation in the bacterial extracellular region.

Best fits of the ten bacterial SERS spectra shown in Fig. 1 resulting from a linear combination of the six component purine spectra (Fig. 5) are displayed in Fig. 6. Excellent fits to all the observed bacterial spectra are achieved by this procedure. Nearly all vibrational features and their relative intensities seen in each of these bacterial SERS spectra are captured by this fitting procedure. Best fits were achieved empirically because of the variable broad spectral background and the small vibrational frequency shifts observed for some bands in the bacterial spectra relative to the aqueous solution component spectra alone as mentioned earlier.

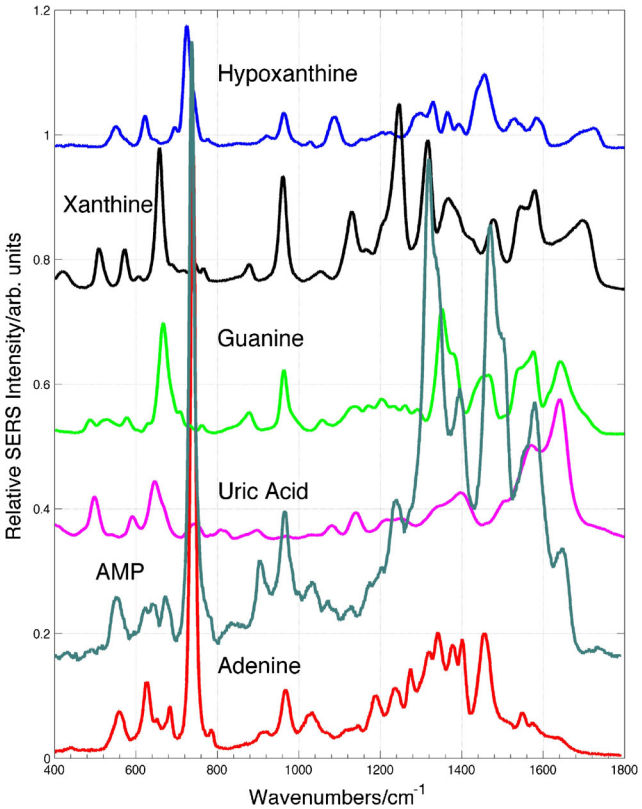

Fig. 5 SERS spectra of 20 μM aqueous solutions of the indicated purine components of bacterial SERS spectra. The spectra have been offset for viewing and are normalized to the maximum peak intensity of the 20 μM adenine solution. *AMP* adenosine monophosphate

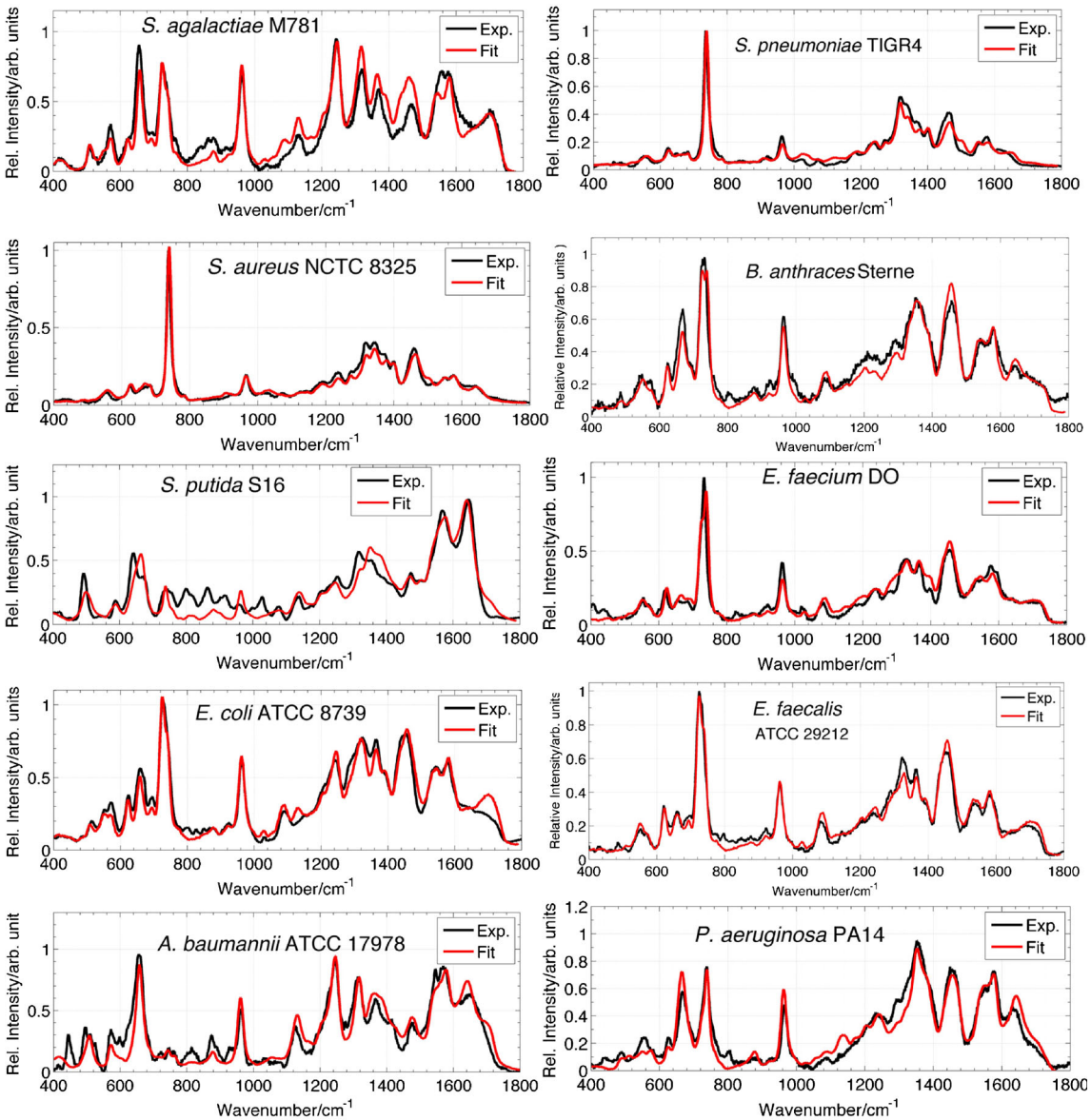

Fig. 6 Empirically determined best fits *(red)* of the bacterial spectra (*black*) shown in Fig. 1 to a linear combination of purine (adenine, hypoxanthine, xanthine, guanine, uric acid, and AMP) SERS spectra shown in Fig. 5. Excellent fits are obtained for all bacterial SERS spectra

Since all bacterial vibrational features result from these small purine molecules and can also be seen in the SERS spectra of the corresponding cell supernatant (Fig. 4), no components of cell walls (i.e., peptidoglycan or any of its constituents, proteins, carbohydrates, or nucleic acids) are required to explain the features evident in these bacterial SERS spectra, and the dominant features in 785-nm SERS spectra can be assigned to a handful of purine molecules. The best-fit-determined relative amounts of the purine components contributing to each of these bacterial spectra are reproducibly different from one another and are summarized in Table 1. For a given purine component, the first number in a purine-specific column Table 1 is the best-fit-determined amplitude of the normalized component SERS spectrum to the observed bacterial spectrum; the second number is the relative contribution corrected by the relative SERS susceptibilities evident in Fig. 5. As seen in Table 1, adenine makes the overwhelmingly dominant contribution to the *Streptococcus pneumonia* TIGR4 and *S. aureus* NCTC 8325 SERS spectra, hypoxanthine makes the largest molecular contribution to the SERS spectra of *B. anthracis* Sterne, *Enterococcus faecium* DO, and *E. faecalis* ATCC 29212, and high uric acid contributions are observed only in the *Pseudomonas putida* S16 and *A. baumannii* ATCC 17978 SERS spectra among this group of organisms. The subsequent distinctions, for example, between the *S. pneumonia* TIGR4 and *S. aureus* NCTC 8325 SERS spectra, result from the different relative amounts of the purines making smaller contributions to these spectra (i.e., the

relative amounts of hypoxanthine, guanine, xanthine, and AMP). As evident from the spectral fitting analysis summarized in Table 1, the different SERS signatures of vegetative bacterial cells are due to the unique characteristic concentration of purines in the extracellular metabolome surrounding the bacterial cells.

Biochemical origins of the SERS spectra of bacteria excited at 785 nm

The SERS spectra of washed vegetative bacterial cells are reproducible vibrational signatures and have been shown for a number of species to be largely independent of typical growth media [57]. The purines contributing to these SERS signatures are the metabolites of purine degradation [58]. The purine metabolic pathways are a highly conserved network of enzymatic reactions in all organisms and are responsible for the degradation of nucleotides and nucleic acids [58]. The end products of these degradation processes in bacteria are the set of purines that are found to dominate the SERS spectra shown here: adenine, hypoxanthine, xanthine, guanine, uric acid, and AMP. The observed SERS spectra of bacteria result from these metabolites that have been secreted during sample preparation and manipulation. The concentration of these molecules is largest in regions closest to the cells from which they are secreted when they are placed on the SERS substrates, but these molecules, which range from slightly soluble to soluble in water, are found in the supernatant solution as well (Fig. 4).

The relative concentration of these purines for each organism is dependent on several factors, but the most crucial appears to be the specific set of enzymes that are present for a given species (strain) in the nucleotide metabolic pathways. The genomically determined absence or presence of specific enzymes accounts for the large range of relative concentration of these purines in the metabolome surrounding these cells and thus determining the SERS spectra obtained with excitation at 785 nm. The enzymes that are present or missing in the purine metabolic pathway for each bacterial species in Fig. 1 are known and are cataloged in the Kyoto Encyclopedia of Genes and Genomes (KEGG) database [58]. The observed SERS spectra of these species (Fig. 1) can be rationalized in terms of these active purine metabolic pathway reactions and the resulting relative purine degradation products.

A diagrammatic representation of the active metabolic pathways is shown in Fig. 7 for six representative bacteria whose SERS spectra are given in Fig. 1. Each box corresponds to a specific nucleotide, nucleoside, or purine base in the degradation of RNA, DNA, or diphosphate or triphosphate nucleotides. The arrows correspond to the enzymes present that convert the indicated product to a reactant. In addition, some enzymes act reversibly depending on the relative concentrations, coenzymes, and other allosteric regulation mechanisms, and are indicated by a double-headed arrow. This reversibility also indicates how this network of enzymatic reactions functions as a purine salvage pathway in addition to a purine degradation pathway. As seen in these purine degradation pathway summaries (Fig. 7), the end products are the free purine bases that dominate the bacterial SERS spectra: adenine, hypoxanthine, xanthine, guanine, and uric acid. Furthermore, this is just a subset of enzymatic reactions that impact the purine metabolic pathways but appear to be most directly linked to the appearance of the main constituents of the SERS spectra reported here [58]. The enzymatic reactions feeding into the nucleoside monophosphate (guanosine monophosphate, xanthosine monophosphate, inosine monophosphate, and AMP) reactants at the top of the diagram are not explicitly included.

As seen in Fig. 7, different combinations of enzymes are present or absent in the metabolic degradation pathways for each of these six bacterial species. The distinct set of active purine metabolism enzymes can be used to explain or at least rationalize the observed different SERS signatures. For example, adenine dominates the *S. aureus* SERS spectrum (Table 1). Correspondingly, adenine-containing nucleotides are metabolized to adenine only by adenine phosphoribosyltransferase for *S. aureus* NCTC 8325 (Fig. 7) [58]. As discussed further later, this is a reversible enzymatic reaction. In contrast to the other metabolic pathways shown in Fig. 7, no enzymes are genetically coded for this organism that permit this nucleotide to be directly converted to inosine or hypoxanthine. *A. baumannii*, on the other hand, has no enzymatic pathways for adenine-containing nucleotides to form adenine (Fig. 7), and hence no adenine is apparent in the SERS spectrum of this organism (Table 1). Instead, reversible enzymatic pathways are available to form guanine, xanthine, hypoxanthine, and uric acid as indicated in Fig. 7, with accumulations of xanthine and uric acid dominating the observed *A. baumannii* SERS spectrum (Table 1). Enzymes are present in *A. baumannii* that can convert hypoxanthine and guanine into xanthine (Fig. 7). In contrast, *P. putida* S16 has the enzymes converting inosine and xanthosine to hypoxanthine and xanthine, and has some ability to produce adenine and guanine. Correspondingly, the *P. putida* S16 SERS spectrum exhibits xanthine, guanine, uric acid, and a very small amount of adenine and AMP. *B. anthracis* is missing the enzymes that convert adenosine to inosine (adenosine deaminase), hypoxanthine to xanthine, and guanine to xanthine (see Fig. 7). Consequently the SERS spectrum of *B. anthracis* is due to large concentrations of hypoxanthine and guanine, and a smaller contribution from adenine (Table 1). The *E. coli* ATCC 8739 and *E. faecalis* ATCC 29212 strains have the enzymes that can interconvert adenine, hypoxanthine, xanthine, and guanine, but this *E. faecalis* strain is missing enzymes that convert xanthosine monophosphate and inosine monophosphate to xanthosine and inosine respectively (Fig. 7). Hypoxanthine makes the largest contribution to the

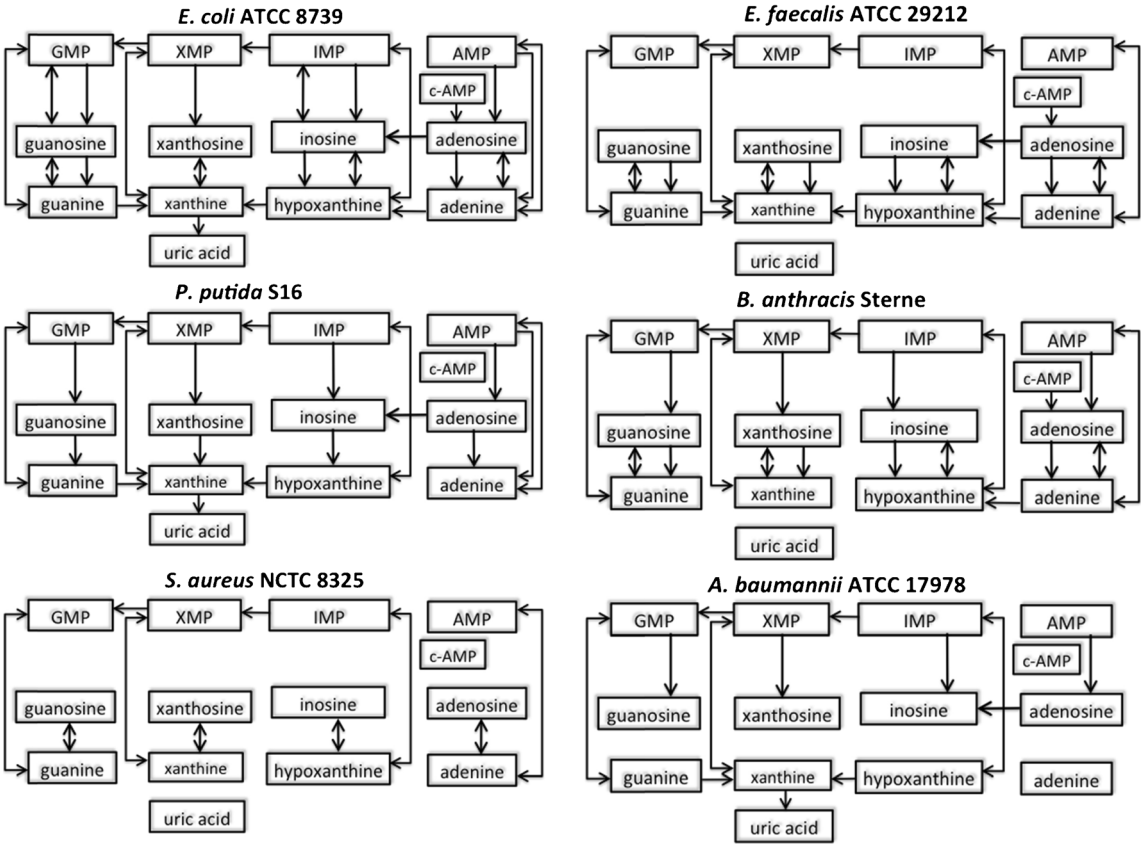

Fig. 7 A subset of the purine metabolic pathways given by the KEGG database [58] for six of the ten bacterial species shown in Fig. 7 that result in the formation of the free nucleobases adenine, hypoxanthine, xanthine, and guanine, and uric acid and AMP. *Single-headed arrows* and *double-headed arrows* correspond to enzymes present for each of the indicated reactions. *c-AMP* cyclic AMP, *GMP* guanosine monophosphate, *IMP* inosine monophosphate, *XMP* xanthosine monophosphate

SERS spectra of both these organisms, with lesser amounts due to xanthine, guanine, and adenine in different proportions, presumably resulting, in part, from the indicated differences in the enzymes present for these two species.

Mass spectra of bacterial supernatants

Since the bacterial supernatant yields nearly the same SERS spectrum as that seen for predominantly cellular samples, we can use mass spectrometry to additionally confirm the absence or presence of molecules in these extracellular solutions and contrast the findings of this method with these SERS results. The mass spectrum in the m/z 100–200 range of the *Streptococcus agalactiae* M781 supernatant wash is displayed in Fig. 8. The most intense features in this lower-mass region are amino acids (valine, leucine, glutamate, phenylalanine) and do not correspond to the purines that dominate the bacterial SERS spectra. Masses corresponding to adenine and hypoxanthine (and xanthine and guanine, not shown here) are more than an order of magnitude weaker than these strongest signals. Furthermore, all the purines that are present (adenine, hypoxanthine, xanthine, and guanine) or absent (uric acid and AMP) in the *S. agalactiae* M781 supernatant SERS spectrum (Table 1) are similarly evident or missing in the corresponding mass spectrum. Analogous results were found for the supernatants of two other bacterial species, *S. aureus* ATCC 25904 and *E. coli* ATCC 8739 (Figs. S1, S2, Table S1), investigated by mass spectrometry. These data illustrate that the molecular susceptibilities for mass spectrometry and SERS are very different and thus these techniques are complementary. Furthermore, the mass spectra data are consistent with the observed bacterial SERS spectra, whose characteristic bands result from the different purines appearing in the bacterial exogenous metabolome.

Effects of genetic mutations on a bacterial SERS spectrum

To further confirm the molecular origins of the bacterial SERS signals and illustrate how SERS may be used as a probe of cellular metabolic reactivity, SERS spectra of a parent *E. coli* strain (BW25113) and two gene-deletion mutants were acquired and are shown in Fig. 9 along with the corresponding best-fit spectra resulting from the linear combination of purine components: adenine, hypoxanthine, xanthine, guanine, uric acid, and AMP. The best-fit-determined relative contributions of these purines to the SERS spectra of these three *E. coli*

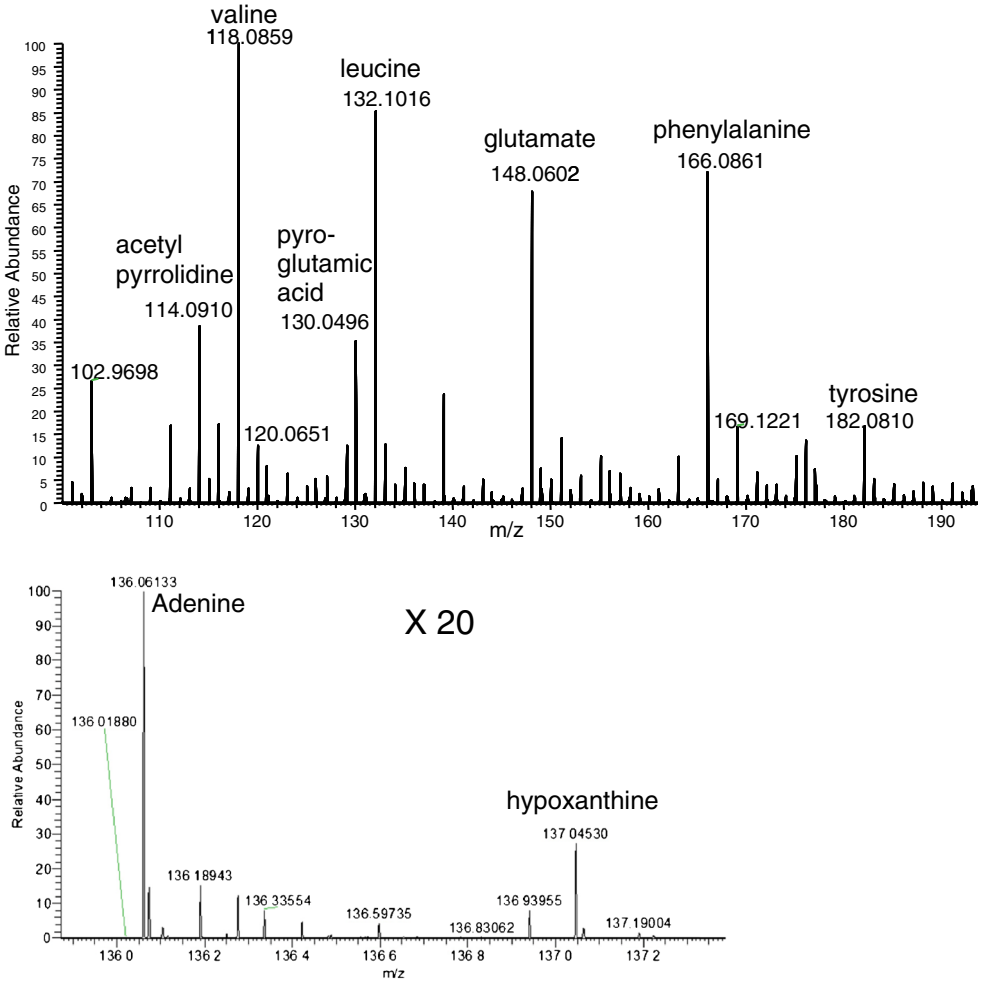

Fig. 8 Positive-ion nano-electrospray ionization mass spectrum of the *Streptococcus agalactiae* M781 supernatant plotted over the *m/z* 120–160 range. The expanded (×20) intensity scale shows *m/z* bands corresponding to adenine and hypoxanthine. Xanthine and guanine were also identified in this mass spectrum. Uric acid and AMP, however, were not evident in this mass spectrum but could be detected in the mass spectra of other samples recorded under the same experimental conditions.. The results are in qualitative agreement with the SERS results (Tables 1, S1)

strains are summarized in Table 2. Hypoxanthine and xanthine make the largest contributions to the observed SERS spectrum of the parent strain, with adenine making a much smaller, although measureable contribution as well. Diagrammatic summaries of the purine metabolic pathways for the parent *E. coli* strain and the two *E. coli* mutants are also shown in Fig. 9. The effect of deletion of the gene encoding adenine deaminase (*ade*), the enzyme converting adenine to hypoxanthine, is relatively small on the SERS signature (Table 2). Interestingly, the effect of deletion of the gene encoding adenosine deaminase (*add*), the enzyme that converts adenosine to inosine (Fig. 9), has a much larger effect on the SERS spectrum than the *ade* deletion, resulting in the appearance of a large amount of adenine in the extracellular metabolome (Table 2). Xanthine and some guanine also contribute to this spectrum, but no significant amount of hypoxanthine is evident in the SERS spectrum of this Δ*add* mutant. In another *E. coli* Δ*add* mutant (CGSC#5937) derived from a different *E. coli* parent strain (CGSC#6925), the Δ*add* SERS spectrum is similarly dominated by adenine, in contrast to the parent SERS spectrum (see Fig. S3, Tables S2a, S2b). Thus, it appears that *add* more efficiently facilitates the formation of hypoxanthine in the adenine nucleotide degradation process as compared with the *ade* reaction pathway. In the *add*-deletion mutants, adenine is secreted to the metabolome more efficiently than *ade* can convert it to hypoxanthine (Figs. 9, S3). This may be attributable to some negative feedback mechanism, allosteric interaction, lack of required coenzyme, or differential kinetic factors (e.g., K_m for *ade* is much larger than K_m for *add* [59]). Furthermore, the small effect on metabolic products resulting from the *ade* deletion is also consistent with previous observations that disruption of the *ade* gene had no obvious phenotypic consequences [60]. SERS spectra of this set of mutants further confirm that the SERS spectra of bacteria excited at 785 nm are not from any cell wall components but are due to the purine end products of nucleotide degradation.

Purine metabolism kinetics

Most observed SERS spectra appear promptly after the water-washed bacterial cells are placed on the SERS substrate and the approximately 1 μL of supernatant water surrounding the suspended cells has evaporated. Signal acquisition has been

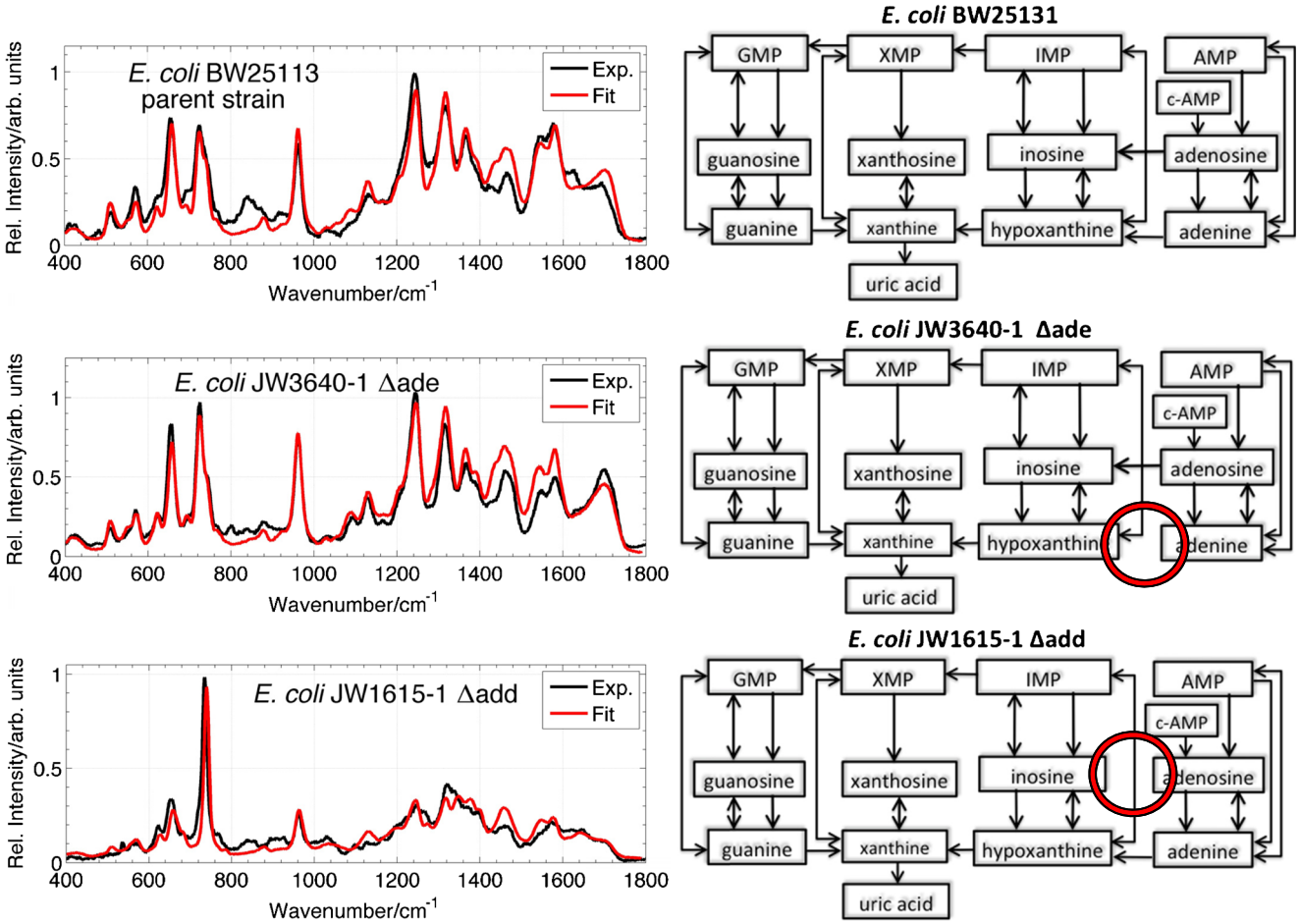

Fig. 9 The SERS spectrum of an *Escherichia coli* parent strain BW25113 and two mutants, JW3640-1 (Δ*ade*) and JW1615-1 (Δ*add*), and their corresponding purine metabolism pathway diagrams

described as prompt, although the four cycles of washing, sample placement, and approximately 1 μL water evaporation take about 15 min. However for *Staphylococcus* and *Streptococcus* species, the maximum signal is not observed until 30–60 min after completion of the washing procedure. A SERS spectrum of *S. aureus* ATCC 25904, observed promptly, designated as $t=0$, and a spectrum of the same bacterial sample after a 60-min delay and maintained at room temperature are plotted on the same relative intensity scale in Fig. 10. A best fit of the $t=60$ spectrum reveals that the SERS spectrum of this *S. aureus* strain is predominantly due to adenine (95 % or greater), with a very small contribution from guanine (5 % or less) (Fig. S4, Table S3). More significantly, however, the $t=60$ min spectrum is approximately 40 times more intense than the $t=0$ spectrum as judged by the relative intensities of the bacterial 736-cm^{-1} adenine band. Adenine phosphoribosyltransferase catalyzes the reversible reaction of AMP to adenine [61], as well as guanosine monophosphate to guanine, in the well-established purine metabolic degradation/salvage network by the reaction in Scheme 1 [58].

The catalyzed transformation of AMP via this degradation step requires diphosphate (diphosphoric acid), forming 5-phospho-α-D-ribose 1-diphosphate and adenine (Scheme 1). When the *S. aureus* cells were washed with a 1 mM solution

Table 2 Best-fit-determined relative (%) purine contributions to an *E. coli* parent strain and two mutants

Organism	Adenine	Hypoxanthine	Xanthine	Guanine	Uric acid	AMP
E. coli BW25113 (parent)	7/2	37/53	56/45	0	0	0
E. coli JW3640-1 (Δ*ade*)	0	48/62	52/38	0	0	0
E. coli JW1615-1 (Δ*add*)	75/53	0	17/34	8/13	0	0

The first number is the percent contribution of the purine component SERS spectrum normalized by the spectrum maximum; the second number is the percent contribution scaled by the relative cross section of the purine component and is thus the relative number of purine component molecules accounting for the SERS signature

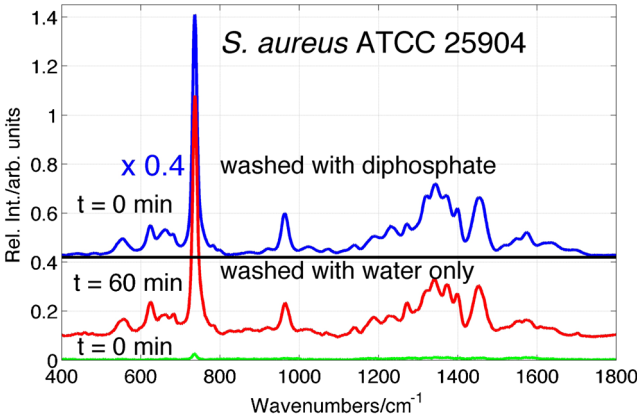

Fig. 10 SERS spectra of *S. aureus* ATCC 25904 as a function of time and as a function of diphosphate exposure. The SERS spectrum appears immediately when the *S. aureus* cells are washed with a 1 mM sodium pyrophosphate solution

of sodium pyrophosphate, forming diphosphate by hydrolysis, an intense prompt SERS spectrum identical to the $t = 60$ min spectrum of water-washed cells was observed as soon as the cells were placed on the SERS substrate and the surrounding water had evaporated (Fig. 10). These data are consistent with the source of the SERS spectrum of *S. aureus* predominantly resulting from the metabolic degradation of AMP. The enzymatic conversion of AMP (and guanosine monophosphate) to adenine (and guanine) has been accelerated by the cellular uptake of the excess diphosphate and thus accounts for the faster rate of adenine appearance in the cell's exogenous metabolome.

Discussion

All of the evidence cited here unequivocally establishes that the SERS spectra of bacterial cells excited at 785 nm are dominated by the reproducible SERS contributions of the free purine nucleobases adenine, hypoxanthine, xanthine, and guanine, and uric acid and AMP. We attribute these observed molecular signals as resulting from the bacterial cell stress response to the no-nutrient, water-only environment they are placed in during sample washing and signal acquisition. In these starvation conditions, it is known that the stringent response of bacterial cells is stimulated [62, 63]. Metabolic rates can change rapidly as the bacterial cell adopts a survival strategy. Cell growth is suspended, and most energy-dependent de novo biosynthesis pathways are turned off. The cell adopts this survival strategy to enable bacteria to persist in stressful environments, reorganizing metabolic activity for both maintenance and survival until conditions potentially become favorable again for the resumption of growth [64, 65]. Nucleobases are not normally present as free bases in the intracellular or extracellular regions but are almost exclusively found as nucleotides under normal nutrient growth conditions.[64] Recent studies have reported increased concentrations of various purines when bacteria are subjected to starvation conditions and their immediate uptake once nutrients are supplied. For example, in a study base on high-performance liquid chromatography, endogenous and exogenous accumulation of nucleobases (xanthine, hypoxanthine, and uracil) was reported in the metabolome of *E. coli* when cells entered the stationary phase [64]. Liquid chromatography–mass spectrometry measurements of *E. coli* metabolites showed dramatic increases of adenine, hypoxanthine, and AMP concentrations following carbon starvation [66]. Most recently, a real-time electrospray ionization time-of flight mass spectrometry study of bacterial cultures injected directly into the mass spectrometer sampling loop revealed purine base (xanthine and hypoxanthine) accumulation during bacterial starvation in the intracellular and extracellular metabolome. These concentrations immediately diminished with the addition of glucose to the nutrient environment [65]. These observations reveal the transient accumulation of exogenous nucleobases during conditions causing declining growth rates, such as nutrient starvation conditions, and are consistent with the SERS results reported here, where spectra were obtained after cells had been enriched from nutrient rich environments and repeatedly washed in pure water before signal acquisition.

Furthermore, the enzymes responsible for the conversion of the purine XMP nucleotides to the base X, such as adenine, guanine, and hypoxanthine phosphoribosyltransferases, are located at the cell membrane and not only facilitate the X ⇔ XMP conversion but also transport these reactants and products across the cell membrane [61, 67, 68]. Hence, the SERS intensities are generally the most intense for excitation of spatial regions closest to the bacterial cell wall. Although the exact details of why secretion of these purines occurs as part

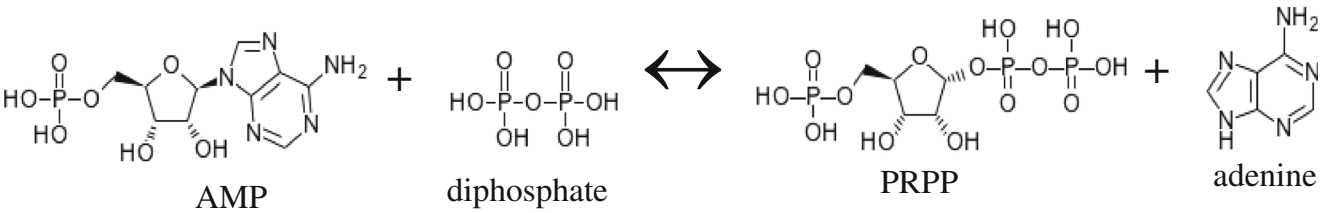

Scheme 1 Adenosine monophosphate (*AMP*) to adenine conversion catalyzed by adenine phosphoribosyltransferase. *PRPP* 5-phospho-α-D-ribose 1-diphosphate

of the starvation response is not clear, it is recognized that nucleotide degradation during starvation is necessary for cell viability [69], and this process has been attributed at least to the degradation of ribosomal RNA as part of the metabolic transformation in response to starvation [64, 69]. It may be speculated that this degradation process provides a low-cost energy source for cell maintenance and survival during the low-nutrient conditions, as well as serving as an instant nitrogen source for the bacterial community once a carbon source or other required nutrients are available. It has been well established that glucose stimulates purine uptake by orders of magnitude in low-nutrient conditions [67], and uptake of purines provides a metabolically cheap one-step salvaging pathway for nucleotide production over the more costly de novo biosynthesis during growth resumption [65].

Conclusions

Conclusive evidence is presented here that clarifies the molecular and biochemical origins of the SERS spectra of bacterial cells excited at 785 nm on Au substrates. The SERS spectra of vegetative bacterial cells harvested from culture medium and washed in water result from the purine bases adenine, xanthine, hypoxanthine, and guanine, as well as uric acid and AMP. These compounds appear at the outer layer of bacterial cells and in the extracellular metabolome, and result from the degradation of nucleotides that occurs as part of the bacterial starvation response. The characteristic SERS spectra are due to the different exogenous concentrations of these six compounds that contribute to each of the bacteria-specific SERS spectra. The observed ^{15}N isotopic vibrational frequency shifts, the near equivalence of SERS spectra of the enriched supernatant and bacterial cells, and the excellent fits of the observed bacterial SERS spectra to linear combinations of the SERS spectra of these six purines unequivocally identify these molecular species as the major constituents that account for the SERS spectra of bacteria excited at 785 nm. These molecular species are secreted from the cells and appear most heavily concentrated in the extracellular regions near the outer cell walls, where purine phosphoribosyltransferases, enzymes that convert purine mononucleotides to purine bases and transport the products across cell membranes, are located. These purines are the end products of the metabolic degradation of nucleic acids and nucleotides, such as RNA, adenosine triphosphate, guanosine triphosphate, and other nucleotide-containing molecules, which rapidly accumulate when bacteria are placed in a nutrient-free environment. Experiments with defined bacterial mutants and substrate perturbation of a purine catalytic pathway further confirm the purine metabolic origin of these bacterial SERS spectra. The rapid exogenous increase in nucleobase concentration is part of the characteristic stringent or starvation response of bacterial cells. The SERS spectra of the bacterial species analyzed here are each unique because of the different amounts of these purine components in this extracellular region, and can be understood in terms of the different enzymes that are present or functional for a given organism. This result is in contrast to the long-held assumption that structural cell wall components, more specifically the peptidoglycan layer components, *N*-acetyl-D-glucosamine, *N*-acetylmuramic acid, lipids, and proteins, make the dominant contribution to the observed SERS spectra at 785 nm and account for their unique characteristic vibrational signature.

Although the SERS spectra of bacteria excited at 514.5 nm/532 nm are strikingly similar to each other, they do not resemble the 785-nm SERS spectra of bacteria as has been noted previously [12, 29, 43]. The SERS spectra of bacteria excited at 514.5 nm/532 nm are nearly equivalent to SERS spectra of FAD [26, 53]. FAD has an electronic absorption in the 350–500-nm region [70] and hence at 514.5 nm/532 nm this molecule will be electronically as well as plasmonically enhanced because of this near resonance [43]. Purine absorptions are further in the UV; hence, the 514.5-nm signature of bacterial SERS is dominated by this single molecule, which provides little basis for diagnostic purposes.

The results described here provide part of the justification for the success of a 785-nm SERS-based method to distinguish different bacterial cell types enriched from culture media or human body fluids for rapid, growth-free infectious disease diagnostics. Whereas many of the observed relative intensities of the bacterial SERS spectral features can be qualitatively rationalized in terms of the absence or presence of specific purine degradation enzymes (Figs. 7 and 9), it remains for future studies to demonstrate the extent that strain-specific diagnostic identification may be robustly accomplished by this SERS-based metabolic profiling approach. Preliminary data acquired in our laboratory point to the ability of this SERS-based method to provide strain specificity classification within some well-defined bacterial classes [31, 71] (Premasiri et al. Rapid, antibiotic specific urinary tract infection diagnostics by surfaceenhanced Raman spectroscopy (SERS), unpublished work).

The bacterial exogenous metabolome is a complex mixture that contains many more compounds [64–66] than the purines that identify these bacterial species via SERS. Since purines dominate the bacterial SERS spectra, the SERS susceptibilities of these compounds must be much larger than those of other molecular components in these mixtures such as leucine, glutamic acid, phenylalanine, valine, arginine, succinic acid, and pyroglutamic acid, which generally appeared with higher signal strength than the purines in mass spectra of bacterial supernatants (Figs. 8, S1, S2). Furthermore, despite the apparent close proximity of the bacterial cell wall, lipids, polysaccharides, peptidoglycan, or protein components of the cell wall structure do not contribute to these bacterial signatures

as well. The Au nanostructured surface apparently has a strong affinity and preferentially interacts with these multiple-nitrogen-containing purines despite the large number of compounds in the cellular environment. It is well known that SERS intensity enhancements are strongly dependent on the details of the surface–analyte interactions [72, 73], and thus the Au nanoparticle structures are selectively enhancing structures for these purine compounds. The Au nanostructured surface not only acts a local Raman amplifier but is also a highly selective filter for a preferential class of small molecules, resulting in the observed purine-dominated SERS spectra of bacteria obtained with 785-nm excitation.

The time-resolved SERS measurements described earlier (Fig. 10) illustrate how real-time SERS measurements can be exploited to monitor the rate of the appearance of this fundamental class of metabolites in the extracellular region and how the kinetics of purine metabolic pathway reactions may be manipulated for studies of factors that affect these metabolic processes and their relationship with other biosynthetic mechanisms and metabolites. As demonstrated here, SERS offers the potential advantages of speed, ease of use, and simpler sample handling protocols with high sensitivity relative to chromatography- or mass-spectrometry-based techniques for metabolomics profiling, at least for some metabolites. Future SERS applications may include examination of the effect of defined bacterial genetic mutants, turnover rates, coenzyme dependence, and the effect of therapeutics on bacterial or cell types either entering or leaving stress environments.

Acknowledgments The support of the National Institutes of Health (grants R01AI090815-01, GM104603, and S10 RR020946) is gratefully acknowledged. We thank Johannes Huebner, Colette Cywes-Bentley, Lawrence Paoletti, Gregory Priebe, Ping Xu, and Fei Tao for providing bacterial strains used in this study and Ying Chen for acquiring the ^{15}N-labeled.

Compliance with ethical standards

Conflict of interest The authors declare that they have no conflict of interest.

References

1. Qian XM, Nie SM. Single-molecule and single-nanoparticle SERS: from fundamental mechanisms to biomedical applications. Chem Soc Rev. 2008;37(5):912–20.
2. Schlücker S. SERS microscopy: nanoparticle probes and biomedical applications. ChemPhysChem. 2009;10(9-10):1344–54.
3. Sharma B, Frontiera RR, Henry A-I, Ringe E, Van Duyne RP. SERS: materials, applications, and the future. Mater Today. 2012;15(1-2):16–25.
4. Premasiri WR, Sauer-Budge AF, Lee JC, Klapperich CM, Ziegler LD. Rapid bacterial diagnostics via surface enhanced Raman microscopy. Spectroscopy (Springf). 2012;27(6):s8–31.
5. Hering K, Cialla D, Ackermann K, Dörfer T, Möller R, Schneidewind H, et al. SERS: a versatile tool in chemical and biochemical diagnostics. Anal Bioanal Chem. 2008;390(1):113–24.
6. Liu T-T, Lin Y-H, Hung C-H, Liu T-J, Chen Y, Huang Y-C, et al. A high speed detection platform based on surface-enhanced Raman scattering for monitoring antibiotic-induced chemical changes in bacteria cell wall. PLoS ONE. 2009;4(5):e5470.
7. Walter A, Marz A, Schumacher W, Rosch P, Popp J. Towards a fast, high specific and reliable discrimination of bacteria on strain level by means of SERS in a microfluidic device. Lab Chip. 2011;11(6):1013–21.
8. Liu T-Y, Tsai K-T, Wang H-H, Chen Y, Chen Y-H, Chao Y-C, et al. Functionalized arrays of Raman-enhancing nanoparticles for capture and culture-free analysis of bacteria in human blood. Nat Commun. 2011;2:538.
9. Nima ZA, Biswas A, Bayer IS, Hardcastle FD, Perry D, Ghosh A, et al. Applications of surface-enhanced Raman scattering in advanced bio-medical technologies and diagnostics. Drug Metab Rev. 2014;46(2):155–75.
10. Cialla D, Pollok S, Steinbrucker C, Weber K, Popp J. SERS-based detection of biomolecules. Nanophotonics. 2014;3(6):383–411.
11. Wu X, Huang Y-W, Park B, Tripp RA, Zhao Y. Differentiation and classification of bacteria using vancomycin functionalized silver nanorods array based surface-enhanced Raman spectroscopy and chemometric analysis. Talanta. 2015;139:96–103.
12. Jarvis RM, Goodacre R. Characterisation and identification of bacteria using SERS. Chem Soc Rev. 2008;37(5):931–6.
13. Efrima S, Bronk BV. Silver colloids impregnating or coating bacteria. J Phys Chem B. 1998;102:5947–50.
14. Efrima S, Bronk BV, Czege J. Surface enhanced Raman spectroscopy of bacteria coated by silver. Proc SPIE. 1999;3602:164–71.
15. Fell Jr NF, Smith AGB, Vellone M, Fountain III AW. Optimization of substrates for surface enhanced Raman spectroscopy of bacteria. Proc SPIE. 2002;4577:174–81.
16. Guzelian AA, Sylvia JM, Janni J, Clauson SL, Spenser KM. SERS of whole cell bacteria and trace levels of biological molecules. Proc SPIE. 2002;4577:182–92.
17. Jarvis RM, Brooker A, Goodacre R. Surface-enhanced Raman spectroscopy for bacterial discrimination utilizing a scanning electron microscope with a Raman spectroscopy interface. Anal Chem. 2004;76(17):5198–202.
18. Jarvis RM, Goodacre R. Discrimination of bacteria using surface-enhanced Raman spectroscopy. Anal Chem. 2004;76(1):40–7.
19. Premasiri WR, Moir DT, Klempner MS, Krieger N, Jones II G, Ziegler LD. Characterization of the surface enhanced Raman scattering (SERS) of bacteria. J Phys Chem B. 2005;109:312–20.
20. Premasiri WR, Moir DT, Ziegler LD. Vibrational fingerprinting of bacterial pathogens by surface enhanced Raman scattering (SERS). Proc SPIE. 2005;5795:19–29.
21. Sengupta A, Laucks ML, Davis EJ. Surface-enhanced Raman spectroscopy of bacteria and pollen. Appl Spectrosc. 2005;59(8):1016–23.
22. Zeiri L, Efrima S. Surface-enhanced Raman spectroscopy of bacteria: the effect of excitation wavelength and chemical modification of the colloidal milieu. J Raman Spectrosc. 2005;36:667–75.
23. Jarvis RM, Brooker A, Goodacre R. Surface-enhanced Raman scattering for the rapid discrimination of bacteria. Faraday Discuss. 2006;132:281–92. discussion 309-19.
24. Guicheteau J, Christesen SD. Principal component analysis of bacteria using surface-enhanced Raman spectroscopy. Proc SPIE. 2006;6218:62180G.
25. Sengupta A, Mujacic M, Davis EJ. Detection of bacteria by surface-enhanced Raman spectroscopy. Anal Bioanal Chem. 2006;386:1379–86.

26. Zeiri L, Bronk BV, Shabtai Y, Eichler J, Efrima S. Surface-enhanced Raman spectroscopy as a tool for probing specific biochemical components in bacteria. Appl Spectrosc. 2004;58:33–40.
27. Laucks ML, Sengupta A, Junge K, Davis EJ, Swanson BD. Comparison of psychro-active Arctic marine bacteria and common mesophillic bacteria using surface-enhanced raman spectroscopy. Appl Spectrosc. 2005;59(10):1222–8.
28. Premasiri WR, Moir DT, Klempner MS, Ziegler LD. Surface enhanced Raman scattering of microorganisms. In: Kneipp K, Aroca R, Kneipp H, Wentrup-Byrne E, editors. New approaches in biomedical spectroscopy. New York: Oxford University Press; 2007. p. 164.
29. Kahraman M, Yazici MM, Sahin F, Bayrak OF, Culha M. Reproducible surface-enhanced Raman scattering spectra of bacteria on aggregated silver nanoparticles. Appl Spectrosc. 2007;61(5): 479–85.
30. Kahraman M, Yazıcı MM, Şahin F, Çulha M. Convective assembly of bacteria for surface-enhanced Raman scattering. Langmuir. 2008;24(3):894–901.
31. Patel IS, Premasiri WR, Moir DT, Ziegler LD. Barcoding bacterial cells: a SERS based methodology for pathogen identification. J Raman Spectrosc. 2008;39(11):1660–72.
32. Culha M, Adiguzel A, Yazici MM, Kahraman M, Sahin F, Gulluce M. Characterization of thermophilic bacteria using surface-enhanced Raman scattering. Appl Spectrosc. 2008;62:1226–32.
33. Chu H, Huang Y, Zhao Y. Silver nanorod arrays as a surface-enhanced Raman scattering substrate for foodborne pathogenic bacteria detection. Appl Spectrosc. 2008;62:922–31.
34. Liu Y, Chen Y-R, Nou X, Chao K. Potential of surface-enhanced Raman spectroscopy for the rapid identification of Escherichia coli and Listeria monocytogenes cultures on silver colloidal nanoparticles. Appl Spectrosc. 2007;61:824–31.
35. Efrima S, Zeiri L. Understanding SERS of bacteria. J Raman Spectrosc. 2009;40(3):277–88.
36. Marotta NE, Bottomley LA. Surface-enhanced Raman scattering of bacterial cell cultural growth media. Appl Spectrosc. 2010;64:601–6.
37. Kahraman M, Zamaleeva AI, Fakhrullin RF, Culha M. Layer-by-layer coating of bacteria with noble metal nanoparticles for surface-enhanced Raman scattering. Anal Bioanal Chem. 2009;395:2559–67.
38. Zhou H, Yang D, Ivleva NP, Mircescu NE, Niessner R, Haisch C. SERS detection of bacteria in water by in situ coating with Ag nanoparticles. Anal Chem. 2014;86(3):1525–33.
39. Kahraman M, Keseroglu K, Culha M. On sample preparation for surface-enhanced Raman scattering (SERS) of bacteria and the source of spectral features of the spectra. Appl Spectrosc. 2011;65:500–6.
40. Felix-Rivera H, Gonzalez R, Rodriguez G, Primera-Pedrozo OM, Rios-Velazquez C, Hernandez-Rivera SP. Improving SERS detection of Bacillus thuringiensis using silver nanoparticles reduced with hydroxylamine and with citrate capped borohydride. Int J Spectrosc. 2011;2011:989504.
41. Culha M, Yazici MM, Kahraman M, Sahin F, Kocagoz S. Surface-enhanced Raman scattering of bacteria in microwells constructed from silver nanoparticles. J Nanotechnol. 2012;2012:297560.
42. Sivanesan A, Witkowska E, Adamkiewicz W, Dziewit L, Kaminska A, Waluk J. Nanostructured silver-gold bimetallic SERS substrates for selective identification of bacteria in human blood. Analyst. 2014;139(5):1037–43.
43. Smith-Palmer T, Douglas C, Fredericks P. Rationalizing the SER spectra of bacteria. Vib Spectrosc. 2010;53(1):103–6.
44. Tettelin H, Nelson KE, Paulsen IT, Eisen JA, Read TD, Peterson S, et al. Complete genome sequence of a virulent isolate of Streptococcus pneumoniae. Science. 2001;293(5529):498–506.
45. Gillaspy AF, Worrell V, Lorvis J, Roe BA, Dyer DW, Iandolo JJ. The Staphylococcus aureus NCTC 8325 genome. In: Fischetti VA, Novick RP, Ferretti JJ, Portnoy DA, Rood JI, editors. Gram-positive pathogens. Washington: ASM Press; 2006. p. 381–412.
46. Yu H, Tang H, Wang L, Yao Y, Wu G, Xu P. Complete genome sequence of the nicotine-degrading Pseudomonas putida strain S16. J Bacteriol. 2011;193(19):5541–2.
47. Lee D, Urbach J, Wu G, Liberati N, Feinbaum R, Miyata S, et al. Genomic analysis reveals that Pseudomonas aeruginosa virulence is combinatorial. Genome Biol. 2006;7(10):R90.
48. Qin X, Galloway-Peña JR, Sillanpaa J, Roh JH, Nallapareddy SR, Chowdhury S, et al. Complete genome sequence of Enterococcus faecium strain TX16 and comparative genomic analysis of Enterococcus faecium genomes. BMC Microbiol. 2012;12:135.
49. Kovacs GJ, Loutfy RO, Vincett PS, Jennings C, Aroca R. Distance dependence of SERS enhancement factor from Langmuir-Blodgett monolayers on metal island films: evidence for the electromagnetic mechanism. Langmuir. 1986;2(6):689–94.
50. Harz M, Rosch P, Peschke KD, Ronneberger O, Burkhardt H, Popp J. Micro-Raman spectroscopic identification of bacterial cells of the genus Staphylococcus and dependence on their cultivation conditions. Analyst. 2005;130(11):1543–50.
51. Rösch P, Schmitt M, Kiefer W, Popp J. The identification of microorganisms by micro-Raman spectroscopy. J Mol Struct. 2003;661–662:363–9.
52. Harz M, Rösch P, Popp J. Vibrational spectroscopy—a powerful tool for the rapid identification of microbial cells at the single-cell level. Cytometry A. 2009;75A(2):104–13.
53. Zeiri L, Bronk BV, Shabtai Y, Czege J, Efrima S. Silver metal induced surface enhanced Raman of bacteria. Colloids Surf A. 2002;208(1–3):357–62.
54. Saikin SK, Olivares-Amaya R, Rappoport D, Stopa M, Aspuru-Guzik A. On the chemical bonding effects in the Raman response: benzenethiol adsorbed on silver clusters. Phys Chem Chem Phys. 2009;11(41):9401–11.
55. Aroca R, Corio P, Rubin JC. Surface enhanced vibrational spectroscopy of 1,2-bis(4-pyridyl) ethane. J Braz Chem Soc. 1996;7:461–9.
56. Kneipp K. Surface enhanced Raman scattering. Phys Today. 2007;40–6
57. Premasiri WR, Gebregziabher Y, Ziegler LD. On the difference between surface-enhanced Raman scattering (SERS) spectra of cell growth media and whole bacterial cells. Appl Spectrosc. 2011;65(5):493–9.
58. Kanehisa M, Goto S. KEGG purine metabolism pathways. 2000. http://www.genome.jp/kegg/pathway/map/map00230.html.
59. BRENDA. The Comprehensive Enzyme Information System. http://www.brenda-enzymes.org/index.php.
60. Petersen C, Møller LB, Valentin-Hansen P. The cryptic adenine deaminase gene of Escherichia coli: silencing by the nucleoid-associated DNA-binding protein, H-NS, AND activation by insertion elements. J Biol Chem. 2002;277(35):31373–80.
61. Berlin RD, Stadtman ER. A possible role of purine nucleotide pyrophosphorylases in the regulation of purine uptake by Bacillus subtilis. J Biol Chem. 1966;241(11):2679–86.
62. Watson SP, Clements MO, Foster SJ. Characterization of the starvation-survival response of Staphylococcus aureus. J Bacteriol. 1998;180(7):1750–8.
63. Kjelleberg S, editor. Starvation in bacteria. New York: Springer; 1993.
64. Rinas U, Hellmuth K, Kang R, Seeger A, Schlieker H. Entry of Escherichia coli into stationary phase is indicated by endogenous and exogenous accumulation of nucleobases. Appl Environ Microbiol. 1995;61(12):4147–51.
65. Link H, Fuhrer T, Gerosa L, Zamboni N, Sauer U. Real-time metabolome profiling of the metabolic switch between starvation and growth. Nat Methods. 2015;12(11):1091–7.

66. Brauer MJ, Yuan J, Bennett BD, Lu W, Kimball E, Botstein D, et al. Conservation of the metabolomic response to starvation across two divergent microbes. Proc Natl Acad Sci U S A. 2006;103(51): 19302–7.
67. Jackman LE, Hochstadt J. Regulation of purine utilization in bacteria. VI. Characterization of hypoxanthine and guanine uptake into isolated membrane vesicles from Salmonella typhimurium. J Bacteriol. 1976;126(1):312–26.
68. Hochstadt-Ozer J, Stadtman ER. The regulation of purine utilization in bacteria: II. Adenine phosphoribosyltransferase in isolated membrane preparations and its role in transport of adenine across the membrane. J Biol Chem. 1971;246(17):5304–11.
69. Kaplan R, Apirion D. The fate of ribosomes in Escherichia coli cells starved for a carbon source. J Biol Chem. 1975;250(5):1854–63.
70. Yagi K, Ozawa T, Harada M. Change of absorption spectrum of flavin adenine dinucleotide by its binding with both D-amino acid oxidase apo-protein and benzoate. Nature. 1959;184(4703):1938–9.
71. Premasiri WR, Lemler P, Chen Y, Gebregziabher Y, Ziegler LD. SERS analysis of bacteria, human blood and cancer cells: a metabolomic and diagnostic tool. In: Ozaki Y, Kneipp K, Aroca R, editors. Frontiers of surface-enhanced Raman scattering: single-nanoparticles and single cells. Chichester: Wiley; 2014. p. 255–82.
72. Le Ru E, Etchegoin P. Principles of surface-enhanced Raman spectroscopy and related plasmonic effects. Amsterdam: Elsevier; 2009.
73. Stiles PL, Dieringer JA, Shah NC, Van Duyne RP. Surface-enhanced Raman spectroscopy. Annu Rev Anal Chem. 2008;1(1):601–26.

W. Ranjith Premasiri is a research scientist (chemistry) at the Photonics Center at Boston University. He is an analytical chemist with expertise in vibrational and surface-enhanced Raman spectroscopy (SERS). He is the inventor of a SERS substrate and portable Raman spectrometer. He is interested in applications of SERS in trace analyses and diagnostics.

Jean C. Lee is Associate Professor of Medicine (infectious diseases) at the Brigham and Women's Hospital and Harvard Medical School. She is a medical microbiologist with specific expertise in the pathogenesis of *Staphylococcus aureus* infections. She has special interests in the staphylococcal capsular polysaccharides, their biosynthesis, function, and regulation, and *S. aureus* vaccine development.

Alexis Sauer-Budge is Head of the Biomedical Group at Fraunhofer Center for Manufacturing Innovation and Adjunct Research Assistant Professor in the Biomedical Engineering Department at Boston University. Her research interests include the development of novel infectious disease diagnostics, tissue engineering, biomedical devices, and scientific instrumentation.

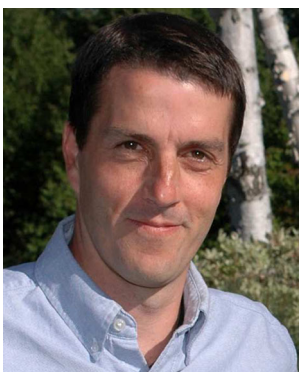

Roger Théberge is a senior research scientist at the Center for Biomedical Mass Spectrometry at the Boston University School of Medicine. He has been working on potential uses of top-down mass spectrometry for the detection and characterization of hemoglobinopathies, and this approach has been adapted to a variety of platforms to evaluate potential clinical applications. His main area of interest is the application of mass spectrometry in the clinical laboratory.

Catherine E. Costello is a William Fairfield Warren Distinguished Professor at Boston University, holding appointments in biochemistry, biophysics and chemistry, and is President of the International Mass Spectrometry Foundation. Her research centers on development and application of mass-spectrometry-based methods to study protein posttranslational modifications and folding disorders, cardiovascular and infectious diseases, Glycobiology, and bioactive lipids.

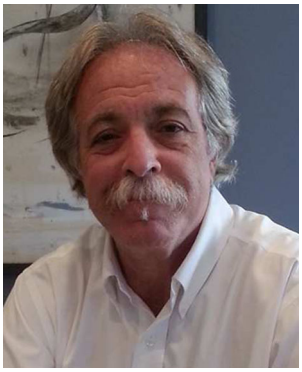

Lawrence D. Ziegler is Professor and Chair of the Department of Chemistry at Boston University and a member of the Boston University Photonics Center. He is also Senior Associate Editor of the *Journal of Raman Spectroscopy*. He has developed a number of novel molecular frequency-domain and time-domain spectroscopic techniques. His current research interests include ultrafast spectroscopic studies of short time dynamics of chemical and materials systems and the development of surface-enhanced Raman spectroscopy for a variety of bioanalytical applications.